

Variable Density Sampling in Compressed Sensing MRI: A Vehicle Routing Approach

Pramit Saha, Satrajit Chakrabarty, Soumya Goswami, Akshay Kumar J, Kasi Rajgopal

Abstract—**k**-space variable density sampling is an effective way of reducing acquisition time in Magnetic Resonance Imaging (MRI). This paper utilizes the notion of compressed sensing by encompassing the variable density sampling problem by a Genetic Algorithm (GA) based Vehicle Routing Problem solver, employed to design an optimal design subspace for perfect reconstruction of sparse signals. Example waveforms are presented for the proposed stochastic drawings, for a variety of design objectives and parameter sets. The methodology has been underpinned by extensive evaluation by various metrics and the results have been compared with several state-of-the-art sampling trajectories.

Index Terms—Compressed sensing, Vehicular Routing Problem, Variable Density Sampling, *k*-space, Hermitian Symmetry, Time Optimal Smoothing

I. INTRODUCTION

Vehicular Routing Problem, formulated mathematically by Dantzig and Ramser [1] is essentially a NP-hard combinatorial optimization problem. Some superior meta-heuristic algorithms have recently been developed, and Genetic Algorithms (GA) have been shown to be capable of solving VRPs [2].

Compressed Sensing [3] in MRI is a theoretical framework which demonstrates the design of a measurement ensemble for accurate reconstruction of incoherent sparse signals, from a limited number of linear sub-Nyquist projections through non-linear and iterative algorithms. CS justifies the possibility of recovering an image from a significantly undersampled Fourier measurement domain of the MR image to overcome the coherence barrier [4] which has culminated in the popularity of *k*-space undersampling using VDS. As most of the energy of an image is concentrated around the *k*-space center in the low-frequency region [3], a VDS may adequately sample the central *k*-space region to reduce low-frequency aliasing artifacts and undersample the outer *k*-space region to reduce scan time and to increase resolution.

In a recent work[5], Chauffert develops an optimal sampling distribution based on independent drawings, in *k*-space with improved image sparsity and sample rejection for any revisited position, that guarantees better reconstruction. The

P. Saha is with the Department of Electrical Engineering, Jadavpur University, Kolkata, India, e-mail: pramitsaha.juee@gmail.com

S. Chakrabarty is with the Department of Electrical Engineering, Jadavpur University, Kolkata, India, e-mail: satrajit2012@gmail.com

S. Goswami is with the Department of Electrical Engineering, Jadavpur University, Kolkata, India, e-mail: soumyagoswami.juee@gmail.com

A. Kumar J is with the Department of Electrical and Electronics Engineering, National Institute of Technology Karnataka, Surathkal, India, e-mail: akshaykumar3495@gmail.com

K. Rajgopal is with the Department of Electrical Engineering, Indian Institute of Science, Bangalore, India, e-mail: kasi@ee.iisc.ernet.in

authors report that the reconstruction quality with heuristic sampling strategies is much better than the theoretical ones owing to the structured image sparsity. The key features of VDS viz. the limit of empirical measures and their mixing properties are elaborated in [6], where the authors have strongly justified the cause of deterministic sampling around the *k*-space centre. In [5], a local random walk sampling based on Markov chains has been presented, enforcing the samples to fit continuous trajectories. But the continuity is strongly dependent on the parameter α in a way that an increase in problem dimension or decrease in continuity offers considerable hardware limitations in MRI, where as an increase in continuity may deteriorate the reconstruction quality. Another continuous trajectory based on global travelling salesman problem (TSP) solver has been employed in [7], that emulates a VDS strategy, but the problem of gradient constraints on MRI scanner still persists. This very problem has been solved in [8], by projecting it onto the set of hardware constraints using convex optimisation, that yields faster trajectories and gives better reconstruction quality at a given scan time.

A closer look reveals certain drawbacks in the TSP strategy. As a single salesman is engaged to traverse all the cities, the movement becomes very chaotic and insignificant without preserving any directional characterisation. Furthermore, the route trajectory imposed on randomly distributed cities leaves the *k*-space centre rarely sampled, deteriorating reconstruction image quality. Hence, there is an inherent urge of extending the TSP solver to an ameliorated approach employing an optimal number of salesmen that may solve these issues. Moreover, incorporating multiple salesman in the form of vehicle routing problem executes the traversing operations parallelly all over the *k* space, enunciating a faster convergence. Since parallel processing or routing is now possible, there is a drastic reduction in acquisition time that serves as a great advantage. As the GA based heuristic solution of the path itself describes a piece-wise linear continuous trajectory, it has been utilized here for semi-perfect sparse MRI reconstruction by reaching a near-optimal solution in minimum number of iterations. An overview of the proposed methodology has been demonstrated with the help of a block diagram in Figure 2.

II. VEHICULAR ROUTING PROBLEM

A. Theory

The Vehicle Routing Problem (VRP) can be described as the problem of designing optimal delivery or collection routes from one or several depots to a number of geographically dispersed destinations (cities or customers) with specific

demands by employing a fleet of vehicles, subject to side constraints. The VRP plays a central role in the fields of physical distribution and logistics. Several variants of the basic problem have been put forward with various constraints such as vehicle capacity, route length, time windows, precedence relations between customers, etc. Strong formulations have been proposed, together with polyhedral studies and exact decomposition algorithms. Most of the research effort has concentrated on a standardized version of the problem, called the classical VRP, with the understanding that many of the algorithms developed for this case, mostly heuristics, can be adapted to suit the more complicated real life situations. The Classical Vehicle Routing Problem (VRP) [9] is one of the most popular problems in combinatorial optimization, and its study has given rise to several exact and heuristic solution techniques of general applicability.

The classical VRP is defined on an undirected graph

$$\begin{aligned} G = (V, A), \text{ where } V &= \{0, 1, \dots, n\}, \\ A &= \{(i, j) : i, j \in V, i \neq j\}, \end{aligned} \quad (1)$$

where V is the vertex set and A is the arc set. Vertex $\{0\}$ represents the initialization depot at which at most m identical vehicles of capacity Q are located. With each customer $i \in V \setminus \{0\}$, a non-negative demand $q_i \leq Q$ is associated. A distance matrix d_{ij} is defined on A . When the distance matrix is symmetric, i.e.,

$$d_{ij} = d_{ji} \forall \{i, j\}, \quad (2)$$

it is common to define the problem on an undirected graph,

$$G = (V, E), \text{ where } E = \{(i, j) : i, j \in V, i < j\}, \quad (3)$$

where E is the edge set. The problem consists of determining a set of m vehicle routes (1) starting and ending at the depot, and such that (2) each customer is visited by exactly one vehicle, (3) the total demand of any route does not exceed Q , and (4) the total routing distance does not exceed a preset limit L . We consider the Vehicle Routing Problem, in which a fixed fleet of delivery vehicles of uniform capacity must service known customer demands for a single commodity from a common depot at minimum transit cost, based on a given distribution of cities and return to their depots forming our desired trajectory, as shown in Figure 1.

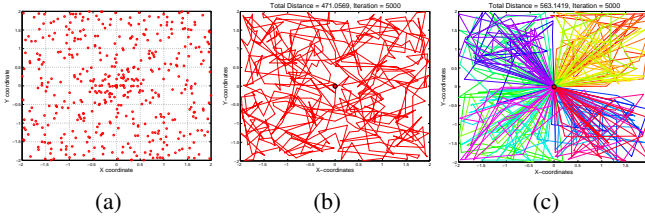


Fig. 1: (a) Distribution of cities, (b)Traversal Route by 1 vehicle, (c) Traversal Route by 100 vehicles

B. Mathematical Framework

The solution of Classical VRP determines a set of delivery routes that is to be traversed by a given set of vehicles

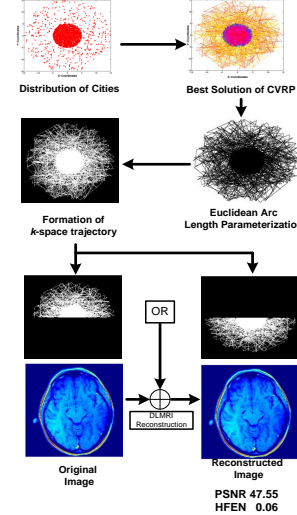


Fig. 2: Schematic of Proposed Methodology.

pertaining to minimization of the total distance travelled. The vehicles are dispatched from a single depot to the distribution points and after delivering goods, are returned to the same point, the number of vehicles remaining user defined and unconstrained and each city being catered by a single vehicle. The mathematical model of the VRP can be expressed as below. Considering total number of vehicles to be m , total number of cities or distribution points or customers n , total capacity of all vehicles Q , capacity of k^{th} vehicle c_k , load requirement at i^{th} distribution point q_i , cost function X_{ij} related with i^{th} and j^{th} distribution points to be distance between i^{th} and j^{th} city, logical assignment condition operators λ_{ij} and μ_{ij} , service time at i^{th} city S_i , maximum traversal time T , traversal time from i^{th} to j^{th} city C_{ij} , the objective function of the problem can be written as,

$$\min \sum_{i=1}^n \sum_{j=1}^n \sum_{k=1}^m \lambda_{ij} X_{ij}, \quad (4)$$

subject to the conditions,

$$\begin{aligned} \sum_{i=1}^n q_i \mu_{ik} &\leq Q, \quad \sum_{i=1}^n q_i \mu_{ik} \leq m c, \quad \sum_{k=1}^m c_k = Q, \\ c_1 = c_2 = c_3 = \dots c_k = c_m = c &= \frac{Q}{m}, \\ \min \sum_{i=1}^n \sum_{j=1}^n \sum_{k=1}^m \lambda_{ij} &\leq m, \quad \sum_{i=1}^n \sum_{j=1}^n \lambda_{ij} = \sum_{i=1}^n \sum_{j=1}^n \lambda_{ji}, \\ \sum_{i=1}^n \lambda_{ij} &= \sum_{i=1}^n \lambda_{ji} = \begin{cases} m, & j = 1 \\ 1, & j = 2, \dots, n \end{cases}, \\ \sum_{k=1}^m \mu_{ik} &= \begin{cases} m, & i = 1 \\ 1, & i = 2, \dots, n \end{cases}, \\ \sum_{i=1}^n \sum_{j=1}^n \lambda_{ij}^k (c_{ij} + S_i) &\leq T^k, \quad k = 1, \dots, m, \\ \sum_{i,j \in S} \lambda_{ij} &\leq |S| - 1, \quad S \subseteq \{2, \dots, n\}, \\ \lambda_{ij}, \mu_{ik} &\in \{0, 1\}, \quad i, j = \{1, \dots, n\}; k = \{1, \dots, m\} \end{aligned} \quad (5)$$

| Algorithm 1: Pseudo-code of proposed methodology | |
|---|--|
| Input : | Reference Image ρ of size $(2N_x + 1) \times (2N_y + 1)$, Coordinate of the depot (C_0), Number(n) and coordinates (C_i) of distribution points, Number of vehicles (m), Minimum tour length for any vehicle (l), Population size($8p$), Allowed number of iterations ($iter$) |
| Output: | Reconstructed Image R of size $(2N_x + 1) \times (2N_y + 1)$ |
| 1 | Initialization of parameters ($P_{initial}$) |
| 2 | Input of user defined parameters($P_{userdefined}$) |
| 3 | Pass user defined parameters to data structure: Indicate the initial configuration structure as the default; |
| 4 | Override any default configuration fields with user values: $P_{initial} \leftarrow P_{userdefined}$ |
| 5 | Initializations for Route Break Point selection: Specify degrees of freedom(F) using $F \leftarrow (n - 1) - l \times m$ |
| 6 | Genetic algorithm function call: $genetic()$; |
| 7 | Return fittest solution trajectory to structure; |
| 8 | Reconstruct the image using modified k -space trajectory; |
| | Function $genetic()$ Input : Parameters and End conditions Output: Fittest solution Initialize Population (random) of routes and breaks using random numbers and global search; Evaluate fitness function; repeat Minimization of infeasible solution; Selection by Roulette Wheel Scheme; Crossover; Mutation using flip, swap, slide operators; Evaluation of fitness function; until end condition is satisfied; Elitism Replacement with filtration; return fittest solution |

Fig. 3: Pseudocode of Proposed Methodology.

$$\lambda_{ij} = \begin{cases} 1, & \text{if } i^{th} \text{ and } j^{th} \text{ city are travelled} \\ & \text{consecutively} \\ 0, & \text{otherwise} \end{cases} \quad (6)$$

$$\mu_{ik} = \begin{cases} 1, & \text{if } i^{th} \text{ city serviced by } k^{th} \\ & \text{vehicle} \\ 0, & \text{otherwise} \end{cases} \quad (7)$$

C. Solution by Genetic Algorithm

The polynomial equation model of the VRP cannot be directly established to determine its optimal solution, and solving time for the VRP grows exponentially with the increase in distribution points. Genetic algorithm being an adaptive heuristic search method that mimics evolution through natural selection has been used in this paper to address VRP which consists in evolving a population of solutions to minimize total travelled distance using genetic operators[2][10].

The search mechanism in GA corresponds to chromosome evolution, comprising reproduction, crossover, and mutation during imitated breeding process. The selection pressure drives the population toward better solutions while recombination uses genes of selected parents to produce offspring that will

form the next generation. Mutation is used to escape from local minima. The population is initialized by a random generation which involves a global search strategy. Initially an evaluation of fitness functions is performed as well as occurrence of infeasible solutions is minimized by removing double trips. The selection procedure is stochastic and biased toward the best solutions using a roulette-wheel scheme which assigns a probability value for selection of an individual proportional to its fitness value. The population size is taken as a multiple of 8 because of the way good solutions in the current population are propagated to the next iteration. Three different mutations are then performed on that best-of-four citizen viz. flip, swap, and slide. Copies of the best-of-four and three mutated versions are made and the lengths of the vehicle routes are mixed up for each. The seven modified solutions are then passed on to the next generation. Eight cities are randomly grouped at a time, the best solution is chosen from them, and it is passed on to the next generation. The proposed algorithm as shown in form of Pseudo-code in Figure 3, has an abstract way of representing possible solutions and turns out to be a method for evaluating the fitness or cost of a candidate solution, a population of candidate solutions, and of propagating good solutions while forming potentially better solutions.

D. Gradient Constraint Fulfilment

We perform a projection of the parameterized curve into an admissible curve as introduced in [11] so that it becomes implementable by actual MRI scanner. The proposed trajectory is first subjected to Euclidean arc length parameterization. Considering that each gradient coil being energized independently, we further impose rotational invariable constraints on the parameterized trajectory. We intend to find an admissible curve subject to minimization of the $\ell^{\infty,2}$ norm at every instant. As a result, the trajectory loses its previous support, and a new support is generated for this smoothed version of the piecewise linear curve. The optimally projected curve on the closed convex constraint set is finally determined using an efficient numerical projection algorithm involving convex optimization which results in time optimal smoothing of the VRP curve around the discrete sampling points or the cities as evident from Figure 4.

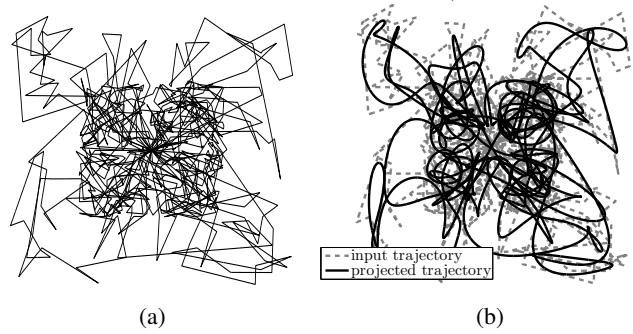


Fig. 4: Figure shows (a) Euclidean Arc Length Parameterization for proposed trajectory, and (b) corresponding RIV smoothed trajectory.

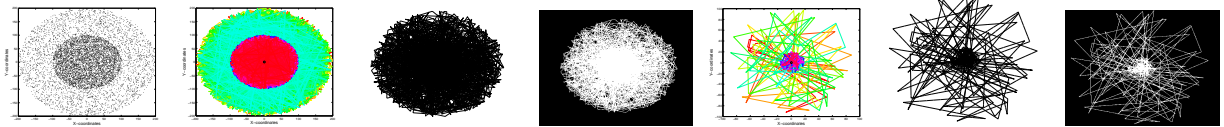


Fig. 5: Figure shows (left-right) random distribution of cities, dense city concentration traversal routes, corresponding generation of trajectory, development of corresponding k-space sampling pattern, rarefied city concentration traversal routes, corresponding generation of trajectory, development of corresponding k-space sampling pattern

III. RESULTS

We have conducted simulations to demonstrate the performance of the proposed k-ABC based VDS scheme for CS-MRI. Dictionary Learning technique (DLMRI) [7] which simultaneously learns an image patch based dictionary and reconstructs the image iteratively using under-sampled data has been used since it shows significantly improved performance over other reconstruction methods. Results of reconstruction were obtained by setting the total number of dictionary learning iterations = 10, number of k-SVD iteration = 20, image patch size = 36 with sparsity T0 = 5 and simulated noise level = 0.005. We considered in-vivo MR scan of brain (Fig. 1(a)) and T2-Weighted Sagittal Spinal image (Fig. 1(b)) as reference images for our simulation. The images are of dimension 512x512. The image quality was evaluated using PSNR (Peak Signal to Noise Ratio), HFEN (High Frequency Normalised Error) and SSIM (Structural Similarity Index Measure), TEI (Transfer Edge Information), Relative ℓ^2 Norm Error (RLNE), Mutual Information (MI) and Blur Metric as metrics for structural fidelity.

Next, we compare the quality of reconstruction from VRP sampling with other VDS sampling schemes for T2-Weighted Sagittal Spinal Image for two under-sampling percentage. The Table II shows the reconstruction quality for R=20% and 5%(in brackets). Our sampling scheme with a PSNR = 49.7 (41.15), HFEN = 0.06(1.29), MSSIM = 0.987(0.952), TEI = 0.91 (0.76), MI = 3.43 (2.79), RLNE = 0.02 (0.05), and Blur Metric = 0.0037 (0.0033) performs significantly better than the independent p-distribution.

A. Experimental Framework

This section discusses the performance of proposed k -space sampling patterns at a variety of undersampling factors both, with and without intrusion of additional noise. The reference MR images that have been used for simulated experiments are of definite sizes: 512×512 , 256×256 , 200×200 , taken from database of American Radiology Services, available online at <http://www.americanradiology.com/>. These in-vivo MR scan images are first subjected to an intensity normalization to a maximum pixel value of 1 and the corresponding Hermitian symmetric 2D k space is obtained by engaging Margolian PF algorithm and consequently subsampled using the proposed sampling patterns. The effectiveness of the sampling masks in reconstruction are justified by comparing the quality of reconstructed image with the other established sampling patterns. The solution is computed using the reconstruction algorithm involving DLMRI [12]. Since our algorithm incorporates the use of random points, we perform a Monte Carlo study that

generates 10 sampling patterns for each of the continuous trajectories produced by the variable density samplers. The implementation of the sampling patterns were coded in Matlab v8.1 (R2013a) and computed with an Intel Core i5 processor at 2.27 GHz and 4GB RAM, employing a 64-bit Windows 7 operating system.

B. Selection of Parameters

The major parameters of the developed trajectory are the concentration of dispersed points in the inner and outer regions, number of active vehicles and number of iterations.

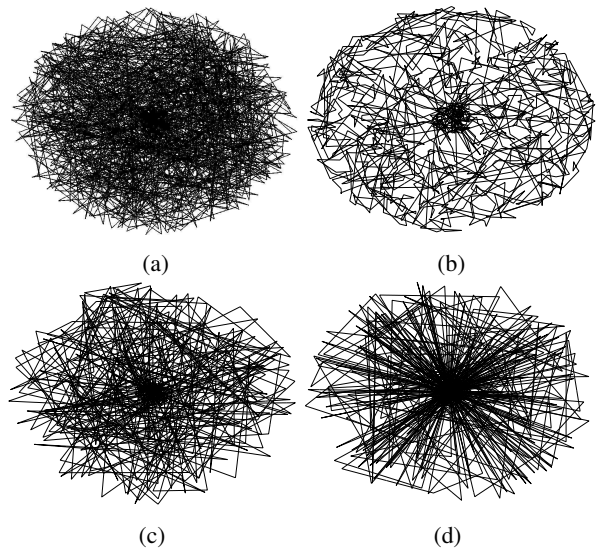


Fig. 6: Generation of trajectory for (a) 100 and (b) 10000 iterations, and (c) 20 and (d) 150 vehicles for identical city distribution and subject to constant other parameters.

From the extensive simulations performed, we observe that the number of iterations act as a decisive factor when the acquisition time is fixed. With an increase of iteration limit as evident from Figure 6(a) and (b), the net distance rapidly decreases and simultaneously, the inter-route criss-cross overlap decreases, that may result in easier parameterisation, reparameterisation and gradient smoothing. But since the chaotic nature of trajectory decreases, there is a corresponding decrease in sampling density over k space. Hence, the iteration number that plays a role in controlling the trade off between these two. The number of iterations are fixed at 5000 for which we achieved optimal results.

For our case, the opposite variation of any one of the vehicle capacity and consumer demand manifests similar effect in the vehicle route. Hence without loss of generality, we

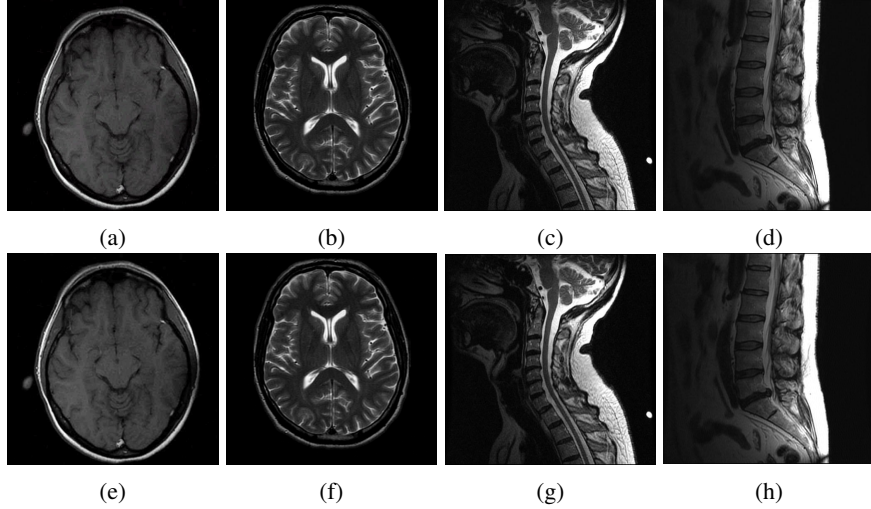


Fig. 7: Figure shows assessment of reconstructed image quality for 20% undersampling for the images (a) In vivo brain image, (b) T2 weighted axial image of brain, (c) T2 weighted sagittal image of spine, and (d) Herniated disc spline. The top row shows the Original images and the bottom row shows the corresponding reconstructed images.

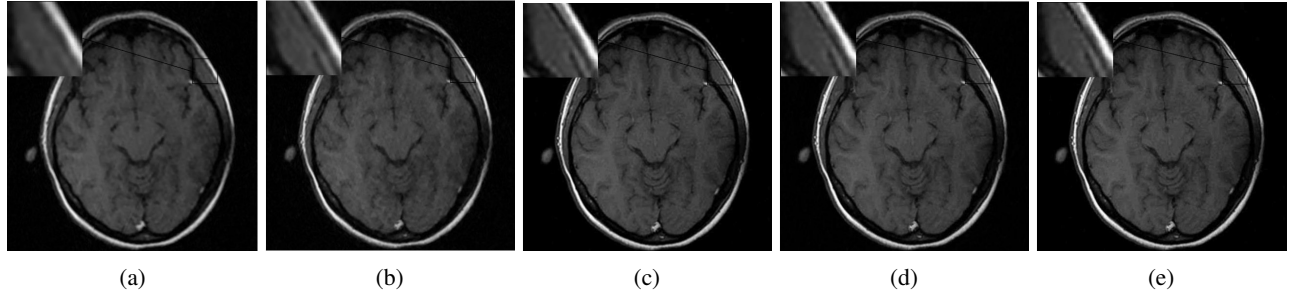


Fig. 8: Figures (a)-(e) show Reconstructed Images for R=20%, 15%, 10%, 6.67% and 5% respectively with magnified region in the top left corner.

may assume the capacity parameter to be constant and vary the demand parameter for reducing complexity of the given problem. A higher value of the consumer demand nearer to the centre depot clearly indicates that more is the probability of the fixed capacity vehicles to traverse short route paths in the centrosymmetric region. This constraint compels the trajectory to be denser near the origin. The optimal distribution of the city demand at any particular location is attained by following a bivariate Gaussian distribution , with zero mean and unit variance, over the k space.

An increment in the central density of k space is also achieved with the increase of available vehicles, as prominent from Figures 6(c) and (d). The figure illustrates that trajectory approaches a radial nature as the number of vehicles go on increasing upto its upper bound, limited by the total number

of sampling points in k space. An empirical rule of selection is assuming the total number of vehicles as half the total number of cities.

The concentration of sampling points or cities are of prime importance in trajectory formation. The inner concentration of points is always kept higher than the outer, in k space. In our simulation, we have emphasised strictly on the incorporation of random points rather than engaging any optimal distribution, because of the results furnished in [6] which demonstrates that heuristic distributions are always advantageous than theoretical ones, due to improved signal sparsity with increase in randomness. Variation in density of distribution of cities imply change in sampling patterns and correspondingly in undersampling ratios as well as reconstruction quality. This has been elaborated in Figure 5.

TABLE I: Evaluation of Reconstruction Quality using different metrics for Optimal parameters for undersamplings of 20%,15%,10% and 5%.

| Undersampling (%) | Parameters | | | | | Evaluation Metrics | | | | | | |
|-------------------|--------------|--------------|--------------|--------------|----------|--------------------|-------|-------|------|------|------|-------------|
| | Outer Radius | Outer Points | Inner Radius | Inner Points | Vehicles | PSNR | HFEN | MSSIM | TEI | MI | RLNE | Blur Metric |
| 20 | 15 | 1000 | 2 | 200 | 50 | 49.7 | 0.06 | 0.987 | 0.91 | 3.43 | 0.02 | 0.0037 |
| 15 | 6 | 300 | 5 | 200 | 100 | 46.2 | 0.146 | 0.974 | 0.88 | 3.32 | 0.03 | 0.0036 |
| 10 | 6 | 1000 | 10 | 50 | 50 | 43.72 | 0.27 | 0.969 | 0.84 | 3.19 | 0.03 | 0.0035 |
| 5 | 16 | 250 | 50 | 30 | 200 | 41.15 | 1.29 | 0.952 | 0.76 | 2.79 | 0.05 | 0.0033 |

C. Performance Evaluation on Test Images

The four references images viz. the coronal section of in vivo Brain Image, T2 weighted axial image of brain, T2 weighted sagittal image of spine, and Herniated disc spline image with their corresponding reconstructed images at five fold undersampling are shown in Figure 7. The figure demonstrates that the images are reconstructed with small distortions and artifacts. The simulation results showing the quality of reconstructed images are extensively summarized in terms of various metrics, in Table I. The parameters selected, are now employed for reconstructing the coronal in vivo brain image corresponding to the specific undersampling values. The reconstructed images are shown in Figure 8, with a magnification on the upper-right boundary region of the brain consisting of sinus, bone, and scalp fat, depicting the capability of the proposed approach to preserve fine details and edges of the constituent parts at varieties of undersampling factors. A discernable increase in the PSNR value of the reconstructed image corresponding to 5% undersampling is conspicuous in the difference image, as shown in Figure 10(c). The performance of the proposed sampling scheme is further

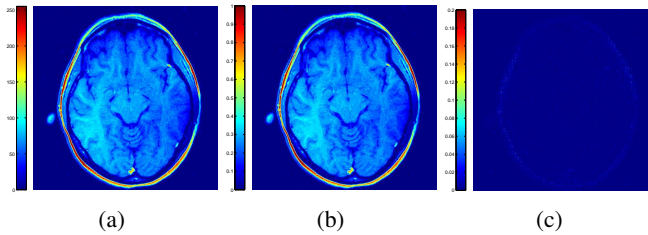


Fig. 10: Figure shows assessment of reconstructed image quality for dorsal view of brain image (512×512) for proposed sampling pattern,(a) Original Brain Image, (b) Reconstructed Images for chosen optimal parameters, and (c) Corresponding Difference Image for DL-MRI.

analysed by plotting the vertical intensity profile of the in vivo brain image for both 5% and 20% undersamplings. While the former shows an overall blurring effect, the edge information is still restored to some extent and the later strictly follows

the image intensities of the input image, which is detailed in the magnified version plotted vertically around (160,160), in the intensity profile.

D. Comparison

Now, for comparison purpose, we also reconstruct the T2 Weighted Spinal Image from other classical and state of the art sampling patterns at an undersampling of 5% and 20% and have been tabulated in Table II. Results clearly show that the proposed strategy of sampling have consistently better performance than other sampling patterns, the performance gain being of maximum 6.66 dB at 20% undersampling, and minimum 5.02 dB at 5% undersampling in terms of PSNR.

TABLE II: Reconstruction Quality of Spinal Image for different VDS Schemes for Undersamplings of 20% and 5%

| VDS Scheme | PSNR | HFEN | SSIM |
|---------------------------------|---------------|-------------|-------------|
| Proposed VRP Scheme | 43.59 (34.21) | 0.46 (3.91) | 0.98 (0.95) |
| Independent π -distribution | 36.93 (29.19) | 1.72 (4.98) | 0.94 (0.84) |
| Power Law based distribution | 32.64 (26.23) | 3.25 (6.61) | 0.89 (0.76) |
| VD-Radial Random Scheme | 33.36 (29.06) | 2.91 (5.08) | 0.92 (0.85) |

IV. DISCUSSION AND PERSPECTIVES

The main purpose of this communication has been to present an alternative view of the sampling process in terms of metaheuristics, that guarantees better reconstruction at higher undersampling.

A visual inspection of the Figure 8(e) testifies that the reconstruction with even 20 fold undersampling, selecting the nominal parameters, are almost free of aliasing and noise. Furthermore, the results indicate that our sampling pattern yield almost 3 times higher reduction factors than the existing methods, at comparable reconstruction errors. The acquisition time is dramatically decreased owing to the notion of parallel sampling and elimination of redundant information in k space.

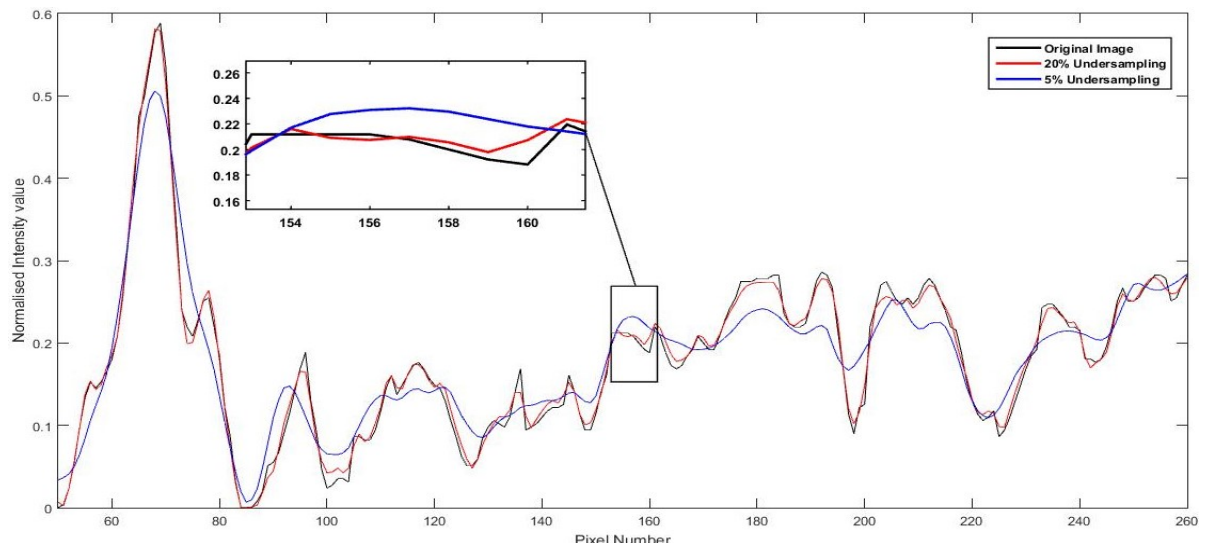


Fig. 9: Intensity Profile Comparison: Along the line $X=160$ and $Y=[50:260]$ shown in Fig. 6(a) of In vivo Brain image

The hermitian symmetry of the sampling pattern in k space, achieved by the conjugate symmetric arrangement of distribution of cities, is beneficial in the respect that it reduces the computational time, enhances the undersampling factor, in a way that the whole pattern can be generated using only the upper half of the entire k space containing the trajectories, thereby eliminating k space redundancy. Though the basic shape of the trajectory remains invariant under rotation (rotating the pattern CW or CCW by 180°, translation (movement of depot) and uniform scaling (expansion or compression of curve), the two latter factors result in changes of sampling pattern and leads to deterioration of reconstructed image quality.

The k space trajectory designed is geometrically stable in a way that a small distortion in the shape of the curve does not alter its representation both in the dense centrosymmetric and rarely sampled high frequency region.

V. CONCLUSION

To the best of our knowledge, this work is the first contribution that addresses VRP with heuristic solution strategy for the design of k space sampling schemes, utilizing the hermitian symmetric property. This rudimentary work investigates the performance of the proposed sampling pattern giving substantially improved reconstruction results than other established patterns, yielding maximum PSNR value of 49.7 at fivefold undersampling. The approach has some additional benefits in the form of parallel sampling, along the trajectory drawn by multiple vehicles at the same time. However the reconstructed image quality at a fixed undersampling depends on the tuning of parameters.

REFERENCES

- [1] G. B. Dantzig and J. H. Ramser, "The truck dispatching problem," *Management science*, vol. 6, no. 1, pp. 80–91, 1959.
- [2] B. M. Baker and M. Aye chew, "A genetic algorithm for the vehicle routing problem," *Computers & Operations Research*, vol. 30, no. 5, pp. 787–800, 2003.
- [3] M. Lustig, D. Donoho, and J. M. Pauly, "Sparse mri: The application of compressed sensing for rapid mr imaging," *Magnetic resonance in medicine*, vol. 58, no. 6, pp. 1182–1195, 2007.
- [4] M. Lustig, D. L. Donoho, J. M. Santos, and J. M. Pauly, "Compressed sensing mri," *Signal Processing Magazine, IEEE*, vol. 25, no. 2, pp. 72–82, 2008.
- [5] N. Chauffert, P. Ciuciu, and P. Weiss, "Variable density compressed sensing in mri. theoretical vs heuristic sampling strategies," in *Biomedical Imaging (ISBI), 2013 IEEE 10th International Symposium on*. IEEE, 2013, pp. 298–301.
- [6] N. Chauffert, P. Ciuciu, J. Kahn, and P. Weiss, "Variable density sampling with continuous trajectories," *SIAM Journal on Imaging Sciences*, vol. 7, no. 4, pp. 1962–1992, 2014.
- [7] ——, "Travelling salesman-based variable density sampling," *arXiv preprint arXiv:1307.6837*, 2013.
- [8] N. Chauffert, P. Weiss, M. Boucher, S. Mériaux, and P. Ciuciu, "Variable density sampling based on physically plausible gradient waveform. application to 3d mri angiography," in *Biomedical Imaging (ISBI), 2015 IEEE 12th International Symposium on*. IEEE, 2015, pp. 1470–1473.
- [9] G. Laporte, M. Gendreau, J.-Y. Potvin, and F. Semet, "Classical and modern heuristics for the vehicle routing problem," *International transactions in operational research*, vol. 7, no. 4–5, pp. 285–300, 2000.
- [10] C.-H. Wang and J.-Z. Lu, "A hybrid genetic algorithm that optimizes capacitated vehicle routing problems," *Expert Systems with Applications*, vol. 36, no. 2, pp. 2921–2936, 2009.
- [11] M. Lustig, S.-J. Kim, and J. M. Pauly, "A fast method for designing time-optimal gradient waveforms for arbitrary-space trajectories," *Medical Imaging, IEEE Transactions on*, vol. 27, no. 6, pp. 866–873, 2008.
- [12] S. Ravishankar and Y. Bresler, "Mr image reconstruction from highly undersampled k-space data by dictionary learning," *Medical Imaging, IEEE Transactions on*, vol. 30, no. 5, pp. 1028–1041, 2011.